PCCP

RSC Publishing

PAPER

View Article Online
View Journal | View Issue

Cite this: *Phys. Chem. Chem. Phys.*, 2013, **15**, 9384

Ultrafast spectroscopy of linear carbon chains: the case of dinaphthylpolyynes†

D. Fazzi,[a] F. Scotognella,[ab] A. Milani,[c] D. Brida,[b] C. Manzoni,[d] E. Cinquanta,‡[e] M. Devetta,[e] L. Ravagnan,[e] P. Milani,[e] F. Cataldo,[f] L. Lüer,[g] R. Wannemacher,[g] J. Cabanillas-Gonzalez,[g] M. Negro,[b] S. Stagira[b] and C. Vozzi*[d]

Received 4th February 2013,
Accepted 19th April 2013

DOI: 10.1039/c3cp50508a

www.rsc.org/pccp

The dynamics of excited states in α,ω-dinaphthylpolyyne, a class of linear sp-carbon chains, has been investigated by ultrafast transient absorption spectroscopy and DFT//TDDFT calculations. We show that the role of molecular conformers, in which end-capped naphthalene rings are planar or perpendicular to the polyyne plane, is fundamental for understanding both the steady state properties, such as UV-Vis absorption spectra and vibronic transitions, and the ultrafast transient absorption features. In particular, we observed in one of the conformers the ultrafast formation of a narrow photo-induced absorption band rising within 30 ps. This band can be assigned to an inter-system crossing event leading to the formation of triplet excited states.

1. Introduction

In the large family of carbon nanostructured materials, sp-carbon systems are particularly interesting owing to their inherent structural simplicity, as well as their peculiar properties, as described in the literature both from the theoretical and the experimental point of view.[1–14] Recently the study of linear carbon chains has attracted the interest of a large number of research groups, because of their unique electronic, optical, and physicochemical properties.[1,3] Linear carbon chains can exist in two idealized isomeric forms namely cumulenes, consisting of double bonds (C=C=C), and polyynes, consisting of alternating quasi single and quasi triple carbon bonds (C–C≡C).[14] Between the two forms, polyyne is predicted to be more stable. Very long polyyne chains, featuring up to 44 carbon atoms and end-capped with bulky terminal groups, have been indeed recently synthesized and characterized by Tykwinski *et al.*[14]

Furthermore, attention has been paid to the interactions of these chains with sp^2 carbon nanodomains[5] and metal nanoparticles[3,15] to further unravel the potentialities of these systems as functional building blocks in nanostructured carbon based materials and in supramolecular chemistry.[3] Linear and nonlinear optical responses of polyynes have been theoretically predicted and experimentally revealed, indicating that sp-hybridized carbon chains behave as true one-dimensional conjugated systems and show large second order hyperpolarizability.[3,4] These findings pave the way for the possible use of polyynes in nonlinear optical applications.

For the understanding of the physicochemical properties of linear carbon chains, investigations based on electronic[16] and vibrational spectroscopy (IR and Raman) are a very powerful tool, owing to the strong electron–phonon coupling that characterizes π-electron conjugated systems.[9,17,18]

On one hand, Raman spectroscopy gives insight into the interplay between bond length alternation, vibrational frequencies and electronic gap in rather long sp-carbon chains,[6,9–12,19,20] and into charge transfer effects upon interaction with metal nanoparticles.[15] On the other hand, IR spectroscopy allows identifying photo-generated cumulenic species resulting from peculiar electronic transitions.[21] A comprehensive interpretation of these experimental results has been allowed by detailed computational studies based on Density Functional Theory (DFT) and Time Dependent DFT (TD-DFT) calculations.[5d,7,22,23] Despite these recent works, many electronic processes in linear

[a] *Center for Nano Science and Technology CNST@Polimi, Istituto Italiano di Tecnologia, via Pascoli 70/3, 20133 Milano, Italy*
[b] *Dipartimento di Fisica, Politecnico di Milano, Piazza L. da Vinci 32, 20133 Milano, Italy*
[c] *Dipartimento di Chimica, Materiali e Ing. Chimica "G. Natta", Politecnico di Milano, Piazza L. da Vinci 32, 20133 Milano, Italy*
[d] *CNR – Istituto di Fotonica e Nanoteconologie, Piazza Leonardo da Vinci 32, 20133 Milano, Italy. E-mail: caterina.vozzi@polimi.it*
[e] *CIMAINA and Dipartimento di Fisica, Università degli Studi di Milano, via Celoria 16, 20133 Milano, Italy*
[f] *Actinium Chemical Research s.r.l., Via Casilina 1626/A, 00133 Roma, Italy*
[g] *IMDEA Nanociencia, C/Faraday 9, 28049 Cantoblanco, Spain*

† Electronic supplementary information (ESI) available. See DOI: 10.1039/c3cp50508a

‡ Present address: Laboratorio MDM, IMM-CNR, Via C. Olivetti 2, 20864 Agrate Brianza (MB), Italy.

carbon chains still need a detailed investigation and understanding. In this framework, ultrafast spectroscopy has been used successfully to study the triplet generation mechanism in polydiacetylene.[24] However, to the best of our knowledge, there are no results in the literature reporting ultrafast spectroscopy studies on polyynic systems.

Here we report on an experimental and theoretical investigation of the photo-physical properties of a class of polyynes, namely α,ω-dinaphthylpolyynes Ar–C_{2n}–Ar, with Ar the naphthyl group and n the number of triple bonds. The experimental results can be interpreted only taking into account the role of the different molecular conformers. Owing to a careful analysis by DFT//TD-DFT calculation we were able to quantify the contributions of each conformer in the UV-Vis absorption spectra. Accordingly ultrafast transient absorption measurements revealed the excited state spectral features and dynamics, as well as the occurrence of inter-system crossing processes. In particular, we observed a selective pathway of triplet formation, determined by the peculiar conformational structure of dinaphthylpolyyne in the ground state.

2. Experimental section

Synthesis of α,ω-dinaphthylpolyynes

Ar–C_{2n}–Ar are synthesized by reacting copper(I)-ethynylnaphthalide with diiodoacetylene under the Cadiot–Chodkiewicz reaction conditions.[25] The obtained batch consists of a mixture of dinaphthylpolyynes having different chain lengths in a decaline solution. Among these, the most abundant species are characterized by n = 1,2,3,4 triple bonds. The concentration of these species is 39.5%mol, 22.9%mol, 25.9%mol and 9.1%mol, respectively. A detailed analysis of the dinaphthylpolyyne mixture has been reported in ref. 25 also in comparison with another chemical route.[26] n = 1 species cannot be considered as a dinaphthyl polyyne like others investigated here (n = 2,3,4) because it features only one end-capped naphthyl group;[25] furthermore, due to its low pi-electron conjugation, n = 1 absorbs at higher energies than n = 2,3,4 thus being out of our spectral range. For these reasons n = 1 has not been considered in this work.

UV-Vis absorption spectra

The absorption spectra of the polyyne n = 2,3,4 were acquired using a liquid chromatograph (HPLC) coupled with a diode array detector.[3,25] By using the diode array detector interfaced to the column of the HPLC, we recorded the electronic absorption spectrum of each molecular species contained in the dinaphthylpolyyne mixture. The identification of each molecular species present in the mixture is based not only on a series of theoretical consideration, but also on the spectra published by Nakagawa and colleagues in an earlier work.[25]

Ultrafast pump–probe measurements

The polyyne mixture (in decaline) was excited with 150 fs pulses centered at 390 nm wavelength, obtained by second harmonic generation from a regeneratively amplified Ti:sapphire laser, operating at 1 kHz. The probe was obtained by focusing a portion of the fundamental beam on a 2 mm thick sapphire plate: self-phase modulation generated supercontinuum white light from 450 to 750 nm. After the interaction with the sample, the probe was coupled to a CCD spectrometer array working at the full repetition rate of the laser. At a given pump–probe delay τ the transient absorption spectrum was retrieved by modulating the pump beam using a mechanical chopper and acquiring each single pump-on/pump-off probe spectrum. The transient signal was calculated as $\Delta T/T(\lambda,\tau) = [T_{ON}(\lambda,\tau) - T_{OFF}(\lambda)]/T_{OFF}(\lambda)$. Upon varying the delay τ by a computer-controlled mechanical translation stage,[27] it was possible to follow the temporal evolution of the transient absorption spectrum $\Delta T/T(\lambda,\tau)$ after the excitation by the pump beam. The temporal resolution of the measurement was limited by the 150 fs pump duration.

Computational methods

DFT and TD-DFT calculations have been carried out on Ar–C_{2n}–Ar systems with n = 2,3,4, using the GAUSSIAN09 code.[28] For each chain length the molecular structure has been fully optimized without constraints in the electronic ground state (S_0), in the first triplet state (T_1) and in the first low lying dipole allowed singlet excited states (S_i). No imaginary vibrational frequencies have been computed for each case thus validating the stability of the equilibrium structures obtained. The hybrid B3LYP[29] exchange–correlation (XC) DFT functional has been combined with different basis sets such as the double split Pople 6-31G** and Dunning's correlation consistent triple-zeta cc-pVTZ basis set. The coulomb attenuated method (CAM-B3LYP)[30] and long range corrected (LC-ωPBE) functional[31] have also been considered for the case of Ar–C_8–Ar (see ESI†). Despite the range separated corrections introduced in CAM-B3LYP and LC-ωPBE functional, for the sp-chain lengths considered here B3LYP turns out to be the best compromise for the description of the electronic structure, as recently suggested in ref. 5*d*, 7, 22, 32 and 33. Due to the large computational demands for calculating both geometries and force fields in different low lying singlet dipole-allowed excited states, we will discuss in the following only B3LYP/6-31G** data. B3LYP/cc-pVTZ calculations for the ground state and excitation energies gave fully equivalent trends with respect to B3LYP/6-31G** data and the results are reported in the ESI.† All calculations have been carried out under *vacuum*, both the molecules and the solvent used for experiments (*i.e.* decalin) being apolar.

For each chain length a conformational analysis has been carried out by varying the dihedral angles (θ_1, θ_2) between the two aryl end-groups, and the meaning of these angles is defined in Fig. 1. Two different ground-state stable conformers have been identified and labeled as (0°, 0°) and (0°, 90°). The (0°, 0°) conformer identifies a chain with the two aryl end-groups in *syn*-conformation (*i.e.* both point in the same direction) while the (0°, 90°) conformer represents a polyyne in which the two aryl end-groups are nearly perpendicular to each other. A further conformer (0°, 180°) can also be defined, but it possesses nearly the same ground and excited state electronic structure of the (0°, 0°) one (see ESI†). For this reason, in the following we will not explicitly consider this conformer.

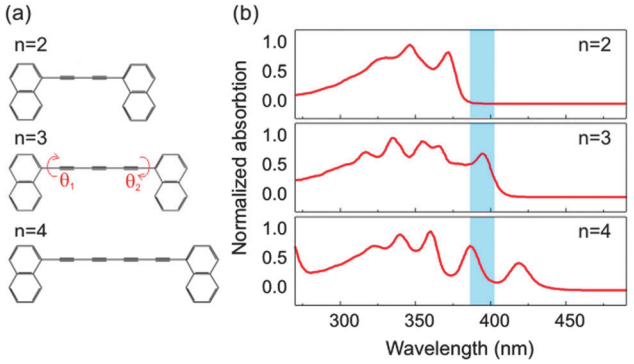

Fig. 1 (a) Chemical structure of Ar–C_{2n}–Ar with n = 2,3,4, where n is the number of triple bonds. (b) Absorption spectra of polyyne with different chain length, the blue shadow indicates the spectral region corresponding to the excitation. θ_1 and θ_2 are the dihedral angles between the two aryl end-groups.

For each stable conformer of the Ar–C_{2n}–Ar series (n = 2,3,4), singlet and triplet excited states have been modeled in the framework of TD-DFT theory and both $S_0 \rightarrow S_i$ and $T_1 \rightarrow T_i$ transitions have been computed (where i indicates a generic electronic excited state).

Singlet excited state geometry optimizations and force field calculations have been carried out at the TD-B3LYP/6-31G** level for each polyyne length and for each molecular conformer. Franck–Condon (FC) factors for the low lying, singlet, dipole allowed excited states have been computed for each transition by using consolidated approaches such as those reported in ref. 34. Absorption spectra have been calculated starting from the TD-DFT FC factors and by performing a convolution with Lorentzian functions with a FWHM of 500 cm^{-1}.

3. Results and discussion

3.1 Steady state analysis: UV-Vis absorption spectra and TD-DFT calculations

An investigation of the electronic absorption spectra of Ar–C_{2n}–Ar has been recently reported in ref. 25 where the main absorption bands have been discussed in terms of FC vibronic progressions. For each polyyne length the dominant vibrational normal modes of the absorption spectra were successfully identified. However, there were features which were still not completely assigned. The absorption spectrum of Ar–C_6–Ar, for example, is different from the other sp-carbon chain systems[16a] and cannot be successfully described by a simple one-mode FC approximation.

In this work we fully investigate the absorption spectra of Ar–C_{2n}–Ar for n = 2,3,4 (see Fig. 1(a)) by explicitly calculating the FC factors at the TD-DFT level. The experimental data are reported in Fig. 1(b). Ground state geometries have been fully optimized using the B3LYP/6-31G** and the molecular structures are reported in the ESI.† For each chain length, the two stable non-degenerate conformers (0°, 0°) and (0°, 90°) have been modeled and the calculated relative energies of the two end-group conformations, $\Delta E(n) = E(0°, 0°) - E(0°, 90°)$, are $\Delta E(2) = -0.24656$ kcal mol^{-1}, $\Delta E(3) = 0.00351$ kcal mol^{-1} and $\Delta E(4) = -0.29746$ kcal mol^{-1}. The very small energy difference between these conformations for all chain lengths suggests that both conformers are thermally populated in solution. Moreover, for the Ar–C_6–Ar the two conformers are practically iso-energetic, with the (0°, 90°) slightly more stable than the (0°, 0°). For both conformers of each chain length TD-DFT vertical excited state calculations have been carried out and the main vertical $S_0 \rightarrow S_i$ transitions are reported in Table 1. These results allow a deeper understanding of the experimental data.

The observed red shift in absorption spectra reported in Fig. 1(b) can be related to the polyyne chain length: longer chains, corresponding to a larger number of sp units, exhibit lower excited state transition energies. The calculated dipole-allowed excited state transitions (see Table 1) can be mainly described, in a single particle approximation, by analyzing the main molecular orbital contributions to the total wave-function and they can be assigned as HOMO → LUMO or HOMO − 1 → LUMO + 1 transitions between orbitals featuring the same spatial π-symmetry ($\Pi_x \rightarrow \Pi_x$, $\Pi_y \rightarrow \Pi_y$).

We now discuss in detail the low-lying excited state landscape of the two stable conformers for each chain length. For the shorter polyyne chains (n = 2,3), the (0°, 0°) conformer presents only *one* dipole-allowed singlet excited state (S_1), while the (0°, 90°) conformer shows *two* low lying dipole-allowed excited states, namely S_1 and S_4 for n = 2 and S_2 and S_4 for n = 3. Furthermore, the energy of the lowest allowed excited states for

Table 1 TD-B3LYP/6-31G** excited state vertical transitions calculated for the first low lying dipole-allowed singlet excited states for Ar–C_{2n}–Ar species, with n = 2,3,4. For each chain length the two stable conformers have been considered namely the (0°, 0°) and the (0°, 90°). TDDFT energies (eV), oscillator strength f and main CI composition are reported (H = HOMO, L = LUMO)

	S_1			S_2			S_3			S_4		
n//conf.	eV	f	CI	eV	f	CI	eV	f	CI	eV	f	CI
2//(0°, 0°)	3.091	0.91	H → L	3.629	0.0	H − 2 → L	3.672	0.0	H − 1 → L H → L + 1	3.919	0.0	H → L + 2
2//(0°, 90°)	3.255	0.34	H → L	3.316	0.0	H → L + 1 H − 1 → L	3.676	0.0	H → L + 1 H − 1 → L	3.801	0.72	H − 1 → L + 1
3//(0°, 0°)	2.844	0.95	H → L	3.087	0.0	H → L + 2 H − 2 → L	3.142	0.0	H → L + 2 H − 2 → L	3.499	0.0	H − 1 → L H → L + 1
3//(0°, 90°)	2.919	0.0	H − 1 → L H → L + 1	2.925	0.20	H → L	3.176	0.0	H − 1 → L H → L + 1	3.505	1.46	H − 1 → L + 1
4//(0°, 0°)	2.597	0.80	H → L	2.645	0.0	H → L + 1	2.754	0.0	H − 1 → L	3.575	0.96	H − 2 → L
4//(0°, 90°)	2.591	0.0	H − 1 → L H → L + 1	2.627	0.07	H → L	2.774	0.0	H − 1 → L H → L + 1	3.258	2.16	H → L+2

the two conformers are slightly different, being S_1 = 3.091 eV (0°, 0°) and 3.255 eV (0°, 90°) for n = 2 and S_1 = 2.844 eV (0°, 0°) and S_2 = 2.925 eV (0°, 90°) for n = 3.

Ar–C_8–Ar species have a similar excited state *scenario*. For this chain length the (0°, 0°) conformer presents two non-negligible excited state transitions to S_1 = 2.597 eV and to S_4 = 3.575 eV. The (0°, 90°) conformer presents two electronic transitions to S_2 = 2.627 eV and to S_4 = 3.258 eV.

Since the conformers are very close in energy, the absorption spectra of Ar–C_{2n}–Ar with n = 2,3,4 should be described as a superposition between the vibronic transitions of both (0°, 0°) and (0°, 90°). In order to verify this hypothesis we computed TD-DFT equilibrium molecular structures and force fields for the dipole-allowed excited states reported in Table 1 by calculating the FC factors and the corresponding vibronic transitions (see ESI† for details and equilibrium structures). The left

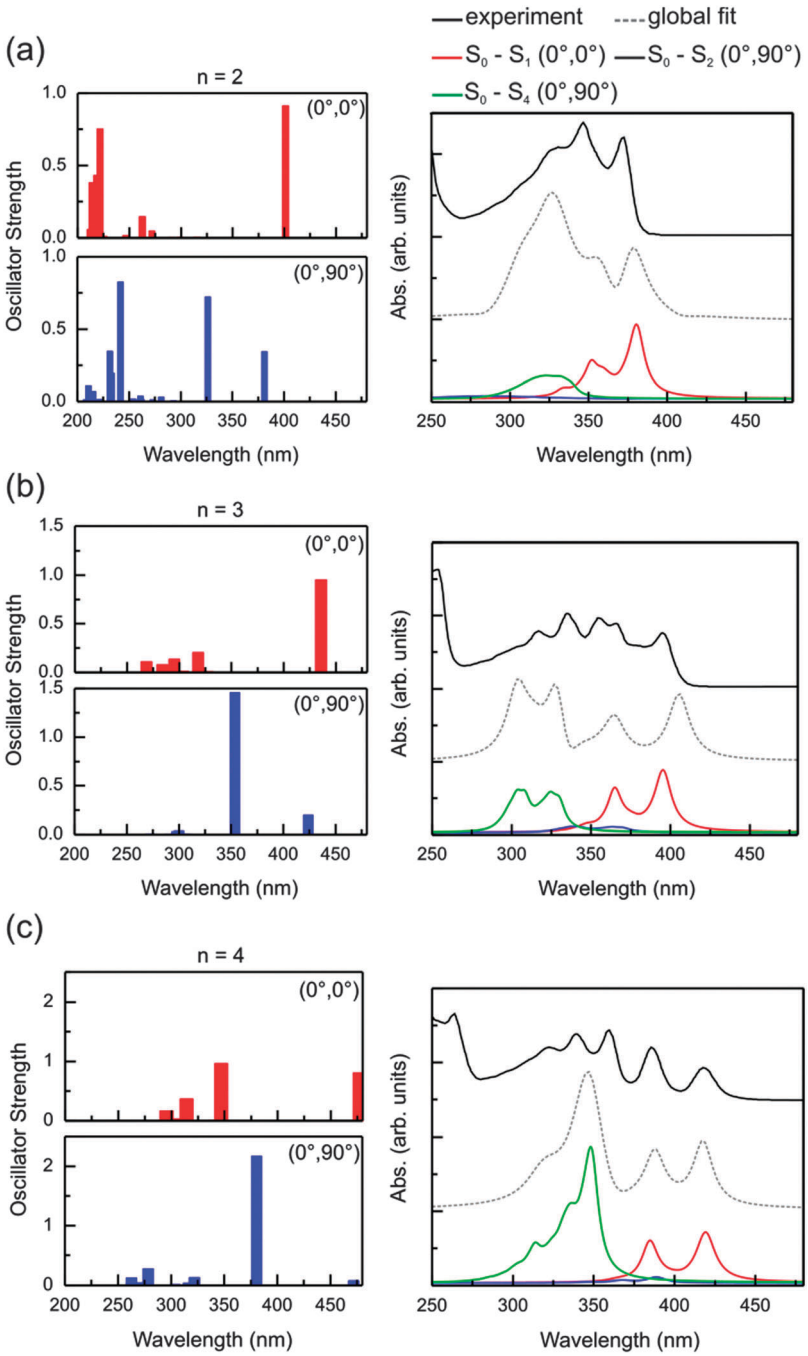

Fig. 2 TD-B3LYP/6-31G** excited state calculations for Ar–C_{2n}–Ar with n = 2,3,4. For each polyyne length we report in the left column: vertical excited state transitions for (0°, 0°) and (0°, 90°) conformers (upper and bottom panels respectively). Right column: calculated absorption vibronic spectra (grey line) as a weight-convolution between the (0°, 0°) and the (0°, 90°) conformer vibronic transitions. Red line is the $S_0 \rightarrow S_1$ transition for (0°, 0°) species while the blue line is the $S_0 \rightarrow S_i$ (i = 1 for n = 2 and i = 2 for n = 3,4) transition and green line is the $S_0 \rightarrow S_4$ transition for (0°, 90°) species. Solid black line, experimental UV-Vis spectra reported for comparison.

column of Fig. 2 shows the calculated excited state transitions for the two conformers of each Ar–C_{2n}–Ar species. In the right panel we show the calculated absorption spectra for each transition (red, green and blue lines) and the corresponding experimental data (black line).[35]

According to Table 1, the following main points can be deduced for all chain lengths: (i) the band in the spectral region 350–450 nm can be assigned to $S_0 \rightarrow S_1$ transition of the (0°, 0°) conformer and to both $S_0 \rightarrow S_1$ and $S_0 \rightarrow S_2$ for the (0°, 90°) conformer; (ii) the bands in the spectral region 320–360 nm can be assigned to transitions related to the $S_0 \rightarrow S_4$ excitation of the (0°, 90°) conformer; (iii) the vibronic structure in the spectral range 370–400 nm can be assigned to a contribution of the $S_0 \rightarrow S_2$ transition of the (0°, 90°) conformer for $n = 3$ and a contribution of the $S_0 \rightarrow S_1$ transition of the (0°, 0°) conformer for $n = 4$.

Indeed, TD-DFT calculations prove that the experimental absorption spectra cannot be interpreted as a vibronic transition of a *unique* molecular species, but the presence of two stable and *quasi*-degenerate conformers has to be taken into account. For each polyyne length, we hence computed the whole absorption spectra as a weighted-convolution of single conformer spectra, shown in Fig. 2 as dashed lines. Such convolution can be expressed as: $s_{tot}(\lambda) = c_a \cdot s_1(\lambda) + c_b \cdot (s_2(\lambda) + s_4(\lambda))$, where $s_1(\lambda)$ is the computed vibronic profile for the (0°, 0°) conformer, $s_2(\lambda)$ and $s_4(\lambda)$ are those of the (0°, 90°) conformer and c_a, c_b are the relative concentration of the two conformers. It is worth noting that c_a contains the contribution of both (0°, 0°) and (0°, 180°) conformers, which are indistinguishable. For evaluating the relative concentration c_a and c_b, we carried out a best fit of the total computed vibronic profile $s_{tot}(\lambda)$ with the experimental absorption spectra. We found for $n = 2$: $c_a = 0.16$ and $c_b = 0.84$, for $n = 3$: $c_a = 0.37$ and $c_b = 0.63$ and for $n = 4$: $c_a = 0.54$ and $c_b = 0.46$. It is worth noting that for $n = 4$ the chain length is long enough to stabilize the flat conformations, which is thus the most abundant in solution. The very good agreement between the calculated TD-DFT absorption spectra and the experiment confirms that the complex and unusual spectral profiles result from the co-presence of the two conformers in the solution.

3.2 Transient absorption spectra and dynamics: the role of triplet states

The aforementioned results pose the basis for understanding the transient absorption experiment.

Fig. 3(a) shows the 2D map of the pump–probe signal. In Fig. 3(b) cuts of the map at different time delays are displayed, while in Fig. 3(c) we show two cuts of the 2D map for two different wavelengths. Over the whole spectral bandwidth it is possible to observe a broad photo-induced absorption, which appears instantaneously upon impulsive photo-excitation. Furthermore, a clear photo-induced absorption signal appears at 600 nm with a time constant of 30 ps and a narrow-band spectral shape (around 20 nm).

It is worth noting that the absorption spectra reported in Fig. 1b reveal that the pump resonantly excited only the polyynes

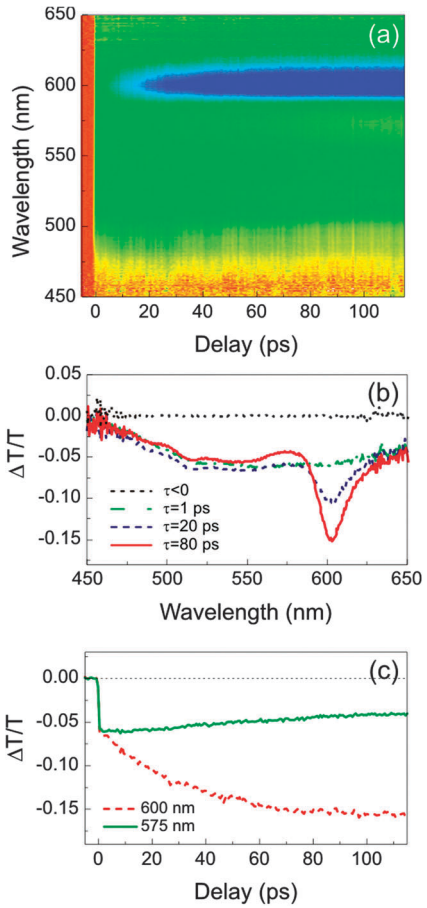

Fig. 3 (a) 2D-map of the pump probe measurement. (b) Contour plot cross sections at different time delays. (c) Transient absorption dynamics for two probe wavelengths: 575 nm (solid curve) and 600 nm (dashed curve).

featuring $n = 3$ and $n = 4$. For this reason, in the following we will restrict our discussion to these polyyne lengths.

In light of DFT//TD-DFT calculations discussed in the following, the observed feature can be assigned to different transitions. In particular, the broad photo-induced absorption, showing a very fast formation time, can be assigned to optical transitions from the excited singlet state to higher molecular singlet levels. On the other hand, the narrow feature centered at 600 nm, characterized by the 30 ps formation time, can be related to an inter-system crossing (ISC) dynamics that leads to the formation of a triplet state followed by transition between triplet states. In this picture the conformers play a prominent role.

We fully optimized the molecular structures in the first triplet excited state at the UB3LYP/6-31G** level (UB3LYP/cc-pVTZ results are reported in the ESI†), which turns out to be flat,[36] with aryl end-groups lying on the same plane. Triplet-to-triplet transitions ($T_1 \rightarrow T_i$) have been evaluated at the TD-(U)DFT level. In Fig. 4 both singlet and triplet TD-DFT excited states are reported. Indeed, the optically allowed triplet-to-triplet transitions have been computed: for $n = 3$, $T_1 \rightarrow T_6$ (1.87 eV, $f = 1.3$) and for $n = 4$, $T_1 \rightarrow T_7$ (1.81 eV, $f = 1.4$). These transitions are in good agreement with the observed photo-induced absorption band, centered at 600 nm. According to

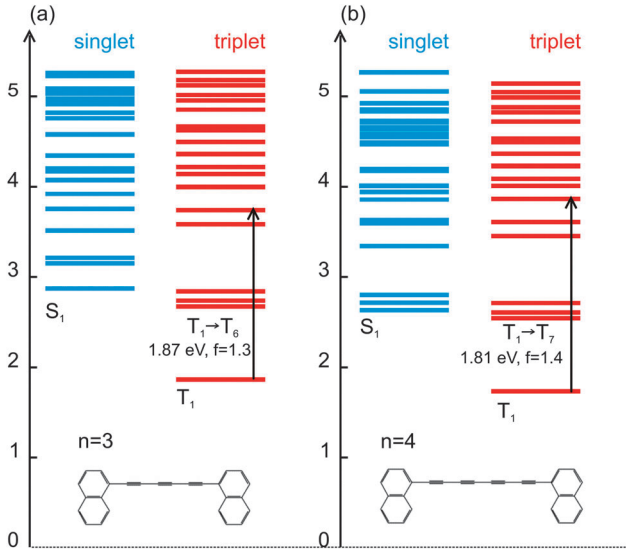

Fig. 4 TD-B3LYP/cc-pVTZ calculated singlet and triplet excited state energies for Ar–C_6–Ar (a) and Ar–C_8–Ar (b). The $T_1 \rightarrow T_n$ dipole allowed transition is also reported in the figure.

TD-DFT calculations, the 600 nm photo-induced absorption signal corresponds to a very narrow-band populated by ISC. Indeed the $T_1 \rightarrow T_6$ (n = 3) and $T_1 \rightarrow T_7$ (n = 4) TD-UDFT transitions are the only dipole-allowed excitations observable in an energy range of 1–5 eV (1240–248 nm) above T_1 (see ESI†).

To sum up, the following photo-physical mechanisms can be hypothesized: (i) the pump laser photo-excites both (0°, 0°) and (0°, 90°) conformers; (ii) once singlet states are populated, singlet-to-singlet transitions can be observed in transient absorption spectra (Fig. 3c); (iii) ISC between singlet and triplet excited states occurs within the first 30 ps.

In Fig. 5 we show the frontier molecular orbitals involved in the description of both the singlet and triplet excited states (z axis defined along the sp-carbon chain) in the case of n = 3. The (0°, 0°) conformer is planar both in the ground state S_0 and

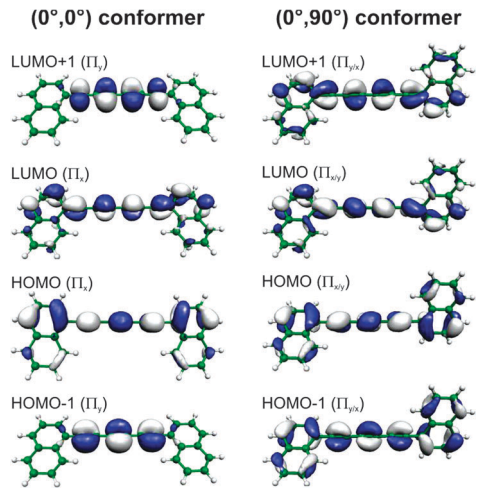

Fig. 5 TD-B3LYP/cc-pVTZ frontier molecular orbitals for Ar–C_6–Ar (0°, 0°) and (0°, 90°) conformers.

in the excited state S_2: the HOMO (LUMO) and HOMO − 1 (LUMO + 1) orbitals are hence orthogonal and present, respectively, a Π_x and a Π_y character, with a C_{2v} point group symmetry. The orthogonal molecular π-orbitals cannot mix, thus preventing ISC. The (0°, 90°) conformer, in contrast, has a distorted molecular structure both in the ground state S_0 and in the optimized dipole-allowed excited state S_2 (see equilibrium ground and excited state structures reported in ESI†). Due to this distorted conformation, featuring the two aryl groups lying on different planes, the local reflection plane (σ_v) is lost, degrading the symmetry of the molecule to a C_2 point group and causing the mixing of the Π_x and Π_y molecular orbitals.[37] A very similar scenario can be depicted for n = 4.

As well reported in the literature, the mixing between two sets of molecular orbitals having different symmetries increases the spin–orbit coupling (the higher is the molecular distortion and the higher is the spin orbit coupling[37]), thus leading to a singlet–triplet excited state non-radiative transition. Therefore, the (0°, 90°) conformer is expected to be the one leading to a more efficient singlet–triplet ISC with respect to the (0°, 0°) conformer. Such analysis of the molecular orbitals confirms that both conformers are excited, but only the (0°, 90°) one decays *via* a non-radiative ISC path toward the T_1 state and is responsible for the photo-induced triplet–triplet band probed at around 600 nm.

The triplet formation leads to a reduction of the broad photo-induced absorption, corresponding to the singlet–singlet transition. This suppression is not complete and the residual signal is then assigned to the singlet–singlet transitions that do not follow the pathway to the ISC process on the ultrafast timescale.

This interpretation is further validated by transient absorption measurements with a pump wavelength of 450 nm. In this case only the (0°, 0°) conformer of the n = 4 polyyne can be excited as can be seen in Fig. 1(b) and the experimental result does not show any absorption band at around 600 nm, which is the signature of ISC (see ESI†). Moreover, we performed nanosecond pump–probe spectroscopy of the sample, pumping at 355 nm and obtaining a strong photoinduced absorption at 600 nm as the only spectral feature in the observed range from 400–1000 nm, characterized by a single exponential life time. Oxygen-induced quenching behaviour strongly suggests that this feature is related to triplet–triplet absorption (see ESI†).

4. Conclusions

In this work, we have studied the photophysical properties of α,ω-dinaphthylpolyynes with different chain lengths by means of electronic and ultrafast pump–probe spectroscopy.

Steady state absorption spectra and DFT//TD-DFT calculations confirmed the presence of two stable *quasi*-degenerate conformers, characterized by different excited state energies and optical activities. In particular, the absorption spectra are interpreted as a superposition between the vibronic transitions of the (0°, 0°) and (0°, 90°) conformers.

We have observed a fast singlet to triplet inter-system crossing mechanism revealed by the formation of a photo-induced

absorption band at 600 nm. TD-DFT calculations assigned the photo-induced band to triplet–triplet excited state transitions. The experimental results, corroborated with the quantum chemical calculations, unravel a selective pathway of triplet formation determined by the conformational structure of the dinaphthylpolyyne molecules in the ground state. In particular, the conformer with the naphthyl end-groups tilted with an angle of 90° shows a non-negligible spin–orbit coupling, allowing an inter-system crossing mechanism to the triplet excited state.

Further experimental and theoretical investigations will pave the way for a more complete understanding of the ultrafast photo-physical *scenario* occurring in exotic organic compounds like polyynes, carbyynes and cumulenes, shedding light on the possible employment of these materials in non-linear optic applications and on the optical manipulation of their physical properties.

Acknowledgements

We acknowledge partial financial support from the Cariplo Foundation through project 2009-2562 and from European Union within contract no. 228334 JRA-ALADIN (Laserlab Europe II) and contract number 248052 FP7-ICT (PHOTOFET). We acknowledge financial support from the Italian Ministry of Research and Education (ELI project – ESFRI Roadmap). JCG and LL thank the Spanish Ministry for Industry and Competitivity for a Ramon y Cajal fellowship and POLYDYE project (TEC2010-21830-C02-02), LL and RW thank the Community of Madrid for financial support (Projects NANOBIOMAGNET, S2009/MAT-1726, and MADRISOLAR2, S2009/PPQ-1533), LL also supported by the EC by the AMAROUT program.

Notes and references

1 (*a*) *Polyynes Synthesis, Properties and Applications*, ed. F. Cataldo, CRC Press, Taylor & Francis, Boca Raton, 2005; (*b*) *Naturally Occurring Acetylenes*, ed. F. Bohlmann, T. Burkhardt and C. Zdero, Academic, New York, 1973; (*c*) *Acetylene Chemistry: Chemistry, Biology, and Material Science*, ed. F. Diederich, P. J. Stang and R. R. Tykwinski, Wiley, Weinheim, 2005; (*d*) *Carbon-Rich Compounds*, ed. M. M. Haley and R. R. Tykwinski, Wiley, Weinheim, 2006, ch. 6; (*e*) R. R. Tykwinski, W. A. Chalifoux, S. Eisler, A. Lucotti, M. Tommasini, D. Fazzi, M. Del Zoppo and G. Zerbi, *Pure Appl. Chem.*, 2010, **82**, 891; (*f*) W. W. Duley and A. Hu, *Astrophys. J.*, 2009, **698**, 808; (*g*) W. A. Chalifoux and R. R. Tykwinski, *C. R. Chim.*, 2009, **12**, 341.

2 S. Szafert and J. A. Gladysz, *Chem. Rev.*, 2003, **103**, 4175.

3 (*a*) A. Lucotti, M. Tommasini, M. Del Zoppo, C. Castiglioni, G. Zerbi, F. Cataldo, C. S. Casari, A. Li Bassi, V. Russo, M. Bogana and C. E. Bottani, *Chem. Phys. Lett.*, 2006, **417**, 78; (*b*) H. Tabata, M. Fujii and S. Hayashi, *Chem. Phys. Lett.*, 2006, **420**, 166; (*c*) H. Tabata, M. Fujii, S. Hayashi, T. Doi and T. Wakabayashi, *Carbon*, 2006, **44**, 3168; (*d*) A. D. Slepkov, F. A. Hegmann, S. Eisler, E. Elliot and R. R. Tykwinski, *J. Chem. Phys.*, 2004, **120**, 6807; (*e*) S. Ballmann, W. Hieringer, D. Secker, Q. L. Zheng, J. A. Gladysz, A. Gorling and H. B. Weber, *ChemPhysChem*, 2010, **11**, 2256; (*f*) D. Nishide, H. Dohi, T. Wakabayashi, E. Nishibori, S. Aoyagi, M. Ishida, S. Kikuchi, R. Kitaura, T. Sugai, M. Sakata and H. Shinohara, *Chem. Phys. Lett.*, 2006, **428**, 356; (*g*) D. Nishide, T. Wakabayashi, T. Sugai, R. Kitaura, H. Kataura, Y. Achiba and H. Shinohara, *J. Phys. Chem. C*, 2007, **111**, 5178; (*h*) C. S. Casari, A. Li Bassi, L. Ravagnan, F. Siviero, C. Lenardi, P. Piseri, G. Bongiorno, C. E. Bottani and P. Milani, *Phys. Rev. B: Condens. Matter Mater. Phys.*, 2004, **69**, 075422; (*i*) L. Ravagnan, P. Piseri, M. Bruzzi, S. Miglio, G. Bongiorno, A. Baserga, C. S. Casari, A. Li Bassi, C. Lenardi, Y. Yamaguchi, T. Wakabayashi, C. E. Bottani and P. Milani, *Phys. Rev. Lett.*, 2007, **98**, 216103; (*j*) C. S. Casari, V. Russo, A. Li Bassi, C. E. Bottani, F. Cataldo, A. Lucotti, M. Tommasini, M. Del Zoppo, C. Castiglioni and G. Zerbi, *Appl. Phys. Lett.*, 2007, **90**, 013111; (*k*) E. Cinquanta, L. Ravagnan, I. E. Castelli, F. Cataldo, N. Manini, G. Onida and P. Milani, *J. Chem. Phys.*, 2011, **135**, 194501; (*l*) C. S. Casari, A. Li Bassi, A. Baserga, L. Ravagnan, P. Piseri, C. Lenardi, M. Tommasini, A. Milani, D. Fazzi, C. E. Bottani and P. Milani, *Phys. Rev. B: Condens. Matter Mater. Phys.*, 2008, **77**, 195444.

4 (*a*) S. Eisler, A. D. Slepkov, E. Elliot, T. Luu, R. McDonald, F. A. Hengmann and R. R. Tykwinski, *J. Am. Chem. Soc.*, 2005, **127**, 2666; (*b*) M. Samoc, G. T. Dalton, J. A. Gladysz, Q. Zheng, Y. Velkov, H. Agren, P. Norman and M. G. Humphrey, *Inorg. Chem.*, 2008, **47**, 9946.

5 (*a*) X. Zhao, Y. Ando, Y. Liu, M. Jinno and T. Suzuki, *Phys. Rev. Lett.*, 2003, **90**, 187401; (*b*) A. Rusznyak, V. Zolyomi, J. Kürti, S. Yang and M. Kertesz, *Phys. Rev. B: Condens. Matter Mater. Phys.*, 2005, **72**, 155420; (*c*) S. Tongay, R. T. Senger, S. Dag and S. Ciraci, *Phys. Rev. Lett.*, 2004, **93**, 136404; (*d*) M. Kertesz and S. Yang, *Phys. Chem. Chem. Phys.*, 2009, **11**, 425.

6 (*a*) A. Milani, M. Tommasini, M. Del Zoppo, C. Castiglioni and G. Zerbi, *Phys. Rev. B: Condens. Matter Mater. Phys.*, 2006, **74**, 153418; (*b*) A. Milani, M. Tommasini, D. Fazzi, C. Castiglioni, M. Del Zoppo and G. Zerbi, *J. Raman Spectrosc.*, 2008, **39**, 164.

7 S. Yang, M. Kertesz, V. Zolyomi and J. Kürti, *J. Phys. Chem. A*, 2007, **111**, 2434.

8 M. Tommasini, D. Fazzi, A. Milani, M. Del Zoppo, C. Castiglioni and G. Zerbi, *J. Phys. Chem. A*, 2007, **111**, 11645.

9 (*a*) A. Milani, M. Tommasini and G. Zerbi, *J. Chem. Phys.*, 2008, **128**, 064501; (*b*) M. Tommasini, A. Milani, D. Fazzi, M. Del Zoppo, C. Castiglioni and G. Zerbi, *Physica E*, 2008, **40**, 2570.

10 A. Milani, M. Tommasini and G. Zerbi, *J. Raman Spectrosc.*, 2009, **40**, 1931.

11 F. Innocenti, A. Milani and C. Castiglioni, *J. Raman Spectrosc.*, 2010, **41**, 226.

12 (*a*) W. Weltner and R. J. Van Zee, *Chem. Rev.*, 1989, **89**, 1713; (*b*) A. Van Orden and R. J. Saykally, *Chem. Rev.*, 1998, **98**, 2313; (*c*) A. L. K. Shi Shun and R. R. Tykwinski, *Angew. Chem., Int. Ed.*, 2006, **45**, 1034.

13 S. Kim, *Angew. Chem., Int. Ed.*, 2009, **48**, 7740.
14 (*a*) W. A. Chalifoux, R. McDonald, M. J. Ferguson and R. R. Tykwinski, *Angew. Chem., Int. Ed.*, 2009, **48**, 7915; (*b*) R. Matsutani, F. Ozaki, R. Yamamoto, T. Sanada, Y. Okada and K. Kojima, *Carbon*, 2009, **47**, 1659; (*c*) W. A. Chalifoux and R. R. Tykwinski, *Nat. Chem.*, 2010, **2**, 967.
15 A. Milani, A. Lucotti, V. Russo, M. Tommasini, F. Cataldo, A. Li Bassi and C. S. Casari, *J. Phys. Chem. C*, 2011, **115**, 12836.
16 (*a*) J. P. Maier, *J. Phys. Chem. A*, 1998, **102**, 3462; (*b*) M. Barbatti, *Wiley Interdiscip. Rev.: Comput. Mol. Sci.*, 2011, **1**, 620; (*c*) F. Plasser, M. Barbatti, A. J. A. Aquino and H. Lischka, *Theor. Chem. Acc.*, 2012, **131**, 1073; (*d*) R. Crespo-Otero and M. Barbatti, *Theor. Chem. Acc.*, 2012, **131**, 1237; (*e*) M. Barbatti, M. Ruckenbauer, J. J. Szymczak, A. J. A. Aquino and H. Lischka, *Phys. Chem. Chem. Phys.*, 2008, **10**, 482.
17 (*a*) G. Zerbi, in *Vibrational Spectroscopy of Polymers: Principles and Practice*, ed. N. J. Everall, J. M. Chalmers and P. R. Griffiths, Wiley, Chichester, 2007, p. 487, and references therein; (*b*) C. Castiglioni, M. Gussoni, J. T. Lopez-Navarrete and G. Zerbi, *Solid State Commun.*, 1988, **65**, 625; (*c*) M. Del Zoppo, C. Castiglioni, P. Zuliani and G. Zerbi, in *Handbook of Conductive Polymers*, ed. T. Skotheim, R. L. Elsembaumer and J. Reynoilds, Dekker, New York, 2nd edn, 1998, p. 765; (*d*) C. Castiglioni, M. Tommasini and G. Zerbi, *Philos. Trans. R. Soc. London, Ser. A*, 2004, **362**, 2425; (*e*) E. Ehrenfreund, Z. Vardeny, O. Brafman and B. Horovitz, *Phys. Rev. B: Condens. Matter Mater. Phys.*, 1987, **36**, 1535.
18 (*a*) D. Fazzi, E. V. Canesi, F. Negri, C. Bertarelli and C. Castiglioni, *ChemPhysChem*, 2010, **11**, 3685; (*b*) R. P. Ortiz, J. Casado, V. Hernández, J. T. López Navarrete, P. M. Viruela, E. Ortí, K. Takimiya and T. Otsubo, *Angew. Chem., Int. Ed.*, 2007, **46**, 9057.
19 A. Lucotti, M. Tommasini, D. Fazzi, M. Del Zoppo, W. A. Chalifoux, M. J. Ferguson, G. Zerbi and R. R. Tykwinski, *J. Am. Chem. Soc.*, 2009, **131**, 4239.
20 L. Ravagnan, N. Manini, E. Cinquanta, G. Onida, D. Sangalli, C. Motta, M. Devetta, A. Bordoni, P. Piseri and P. Milani, *Phys. Rev. Lett.*, 2009, **102**, 245502.
21 M. M. Yildizhan, D. Fazzi, A. Milani, L. Brambilla, M. Del Zoppo, W. Chalifoux, R. R. Tykwinski and G. Zerbi, *J. Chem. Phys.*, 2011, **134**, 124512.
22 S. Yang and M. Kertesz, *J. Phys. Chem. A*, 2008, **112**, 146.
23 B. Xi, I. P. C. Liu, G. L. Xu, M. M. R. Choudhuri, M. C. DeRosa, R. J. Crutchley and T. Ren, *J. Am. Chem. Soc.*, 2011, **133**, 15094–15104.
24 G. Lanzani, G. Cerullo, M. Zavelani-Rossi, S. De Silvestri, D. Comoretto, G. Musso and G. Dellepiane, *Phys. Rev. Lett.*, 2001, **87**, 187402.
25 F. Cataldo, L. Ravagnan, E. Cinquanta, I. E. Castelli, N. Manini, G. Onida and P. Milani, *J. Phys. Chem. B*, 2010, **114**, 14834.
26 M. Nakagawa, S. Akiyama, K. Nakasuji and K. Nishimoto, *Tetrahedron*, 1971, **27**, 5401.
27 D. Brida, C. Manzoni, G. Cirmi, D. Polli and G. Cerullo, *IEEE J. Sel. Top. Quantum Electron.*, 2012, **18**, 329.
28 M. J. Frisch, *et al.*, *Gaussian 09, revision A.1*, Gaussian, Inc., Wallingford, CT, 2009.
29 A. D. Becke, *J. Chem. Phys.*, 1993, **98**, 1372.
30 T. Yanai, D. Tew and N. Handy, *Chem. Phys. Lett.*, 2004, **393**, 51–57.
31 O. A. Vydrov and G. E. Scuseria, *J. Chem. Phys.*, 2006, **125**, 234109.
32 M. Kertesz, C. H. Choi and S. Yang, *Chem. Rev.*, 2005, **105**, 3448–3481.
33 S. Yang and M. Kertesz, *J. Phys. Chem. A*, 2006, **110**, 9771–9774.
34 (*a*) E. Di Donato, D. Vanzo, M. Semeraro, A. Credi and F. Negri, *J. Phys. Chem. A*, 2009, **113**, 6504; (*b*) F. Negri and M. Z. Zgierski, *J. Chem. Phys.*, 1994, **100**, 1387; (*c*) F. Negri and M. Z. Zgierski, *J. Chem. Phys.*, 1994, **100**, 2571; (*d*) F. Negri and G. Orlandi, *J. Phys. B: At., Mol. Opt. Phys.*, 1996, **29**, 5049; (*e*) F. Santoro, R. Improta, A. Lami, J. Bloino and V. Barone, *J. Chem. Phys.*, 2007, **126**, 084509; (*f*) F. Santoro, A. Lami, R. Improta and V. Barone, *J. Chem. Phys.*, 2007, **126**, 184102; (*g*) V. Barone, J. Bloino, M. Biczysko and F. Santoro, *J. Chem. Theory Comput.*, 2009, **5**, 540; (*h*) F. Santoro, R. Improta, A. Lami, J. Bloino and V. Barone, *J. Chem. Phys.*, 2008, **128**, 224311.
35 For Ar–C_8–Ar the energies of $S_0 \rightarrow S_4$ $(0^\circ, 0^\circ)$ and $(0^\circ, 90^\circ)$ are well overlapped. We considered the latter to be dominant due to the highest oscillator strength, as reported in Table 1.
36 The $(0^\circ, 90^\circ)$ conformer in T_1 indeed relaxes in a $(0^\circ, 180^\circ)$ conformation, whose electronic properties are practically equivalent to the $(0^\circ, 0^\circ)$ one, as indicated above.
37 D. Beljonne, Z. Shuai and J. L. Bredas, *J. Phys. Chem. A*, 2001, **105**, 3899.